International Food Research Journal 32(3): 789 - 799 (June 2025)

Journal homepage: http://www.ifrj.upm.edu.my



Effect of high-intensity ultrasounds at different power levels on structural properties and foam stability of quinoa protein

¹Huang, P. and ²*Bu, K.-X.

¹Jinan Food and Drug Testing Center, Jinan Shandong 250102, P. R. China ²College of Food Science and Engineering, Key Laboratory of Food Processing Technology and Quality Control in Shandong Province, Shandong Agricultural University, Taian 271018, P. R. China

Article history

Received: 27 July 2024 Received in revised form: 8 May 2025 Accepted: 3 June 2025

Keywords

quinoa protein, ultrasound, foam, structure modification, interfacial properties

Abstract

Quinoa, an ancient cereal crop with a long cultivation history and rich in protein, faces limitations due to its proteins having naturally poor water solubility, which limits their foaming properties in the food processing industry. This may be due to the extensive formation of soluble aggregates during the protein extraction process. Therefore, the present work utilised high-intensity ultrasounds (HIUS) to modify quinoa protein (QP). The present work systematically investigated the effect of ultrasound on the fundamental properties, secondary structure, and tertiary structure of QP. Additionally, it explored the impact of changes in QP properties and structure on its solubility and foam properties. The treated QP exhibited significantly improved solubility and foam properties. Following HIUS treatment, the solubility of QP increased from 10.59 to 57.86%, and its foaming capacity also improved significantly, increasing from 47.56 to 107.24%, providing theoretical guidance for future applications.

DOI

https://doi.org/10.47836/ifrj.32.3.13

© All Rights Reserved

Introduction

Nowadays, with the rapid expansion of the population, consumers' demand for foods has gradually shifted from "eating sufficiently" to "eating healthily". As a result, the demand for protein has also increased dramatically. Compared to animal-based proteins with long growth cycles, and higher greenhouse gas emissions, plant-based protein may be an optimal solution. Quinoa, originating from the Andes Mountains, is an ancient and important cereal with high protein content, reaching up to 15%, surpassing other grains. Quinoa protein (QP) not only has a balanced amino acid composition, including all essential amino acids, but is also gluten-free, making it suitable for individuals with gluten sensitivity (Wang et al., 2024). Recent studies have shown that QP exhibited good anti-inflammatory and antioxidant activities. Additionally, it can reduce the incidence of type II diabetes by inhibiting carbohydrate digestion. It is considered a high-quality protein supplement (Cui et al., 2023). Therefore, it is hoped that the abundant and high-quality protein resources in quinoa can be utilised in the food industry.

The functional properties of proteins determine their limits in the food industry (Kong et al., 2023). Foaming, gelling, and emulsifying properties are crucial for the application of proteins in various food products. Foaming, as one of the essential functional properties, has been widely utilised in aerated foods, cakes, bread, and more. With the advancements in food processing, food companies aim to enhance product texture, and increase consumer purchasing desire by utilising the foaming properties of proteins (Yang et al., 2022). Compared to animal-based proteins, plant-based proteins like QP have a natural disadvantage in application due to factors such as poor solubility, which significantly affects their interfacial properties, and consequently foam characteristics. Various technologies, including ultrasound, high-pressure homogenisation, treatment, enzymatic modification, glycosylation, etc., have been applied to modify protein functionality (Nasrabadi et al., 2021). Compared with

*Corresponding author. Email: bkxsdau@163.com other treatment methods, ultrasound processing offers advantages such as cleanliness, high efficiency, and no pollution, making it highly suitable for large-scale protein modification.

High-intensity ultrasounds (HIUS), as a nonthermal processing technique, is safe, non-toxic, and energy-efficient, attracting considerable attention in protein modification. In the research conducted by Du et al. (2022), ultrasound-induced cavitation altered the secondary and tertiary structures of pumpkin-seed protein isolates, thereby improving their foaming properties. In Fu's experimental study (Fu et al., 2022), ultrasound increased the foaming capacity of cottonseed protein isolate from 38.88 to 83.80% and enhanced its emulsifying ability from 13.04 to 25.04. The poor solubility of QP severely hampers its foam properties for food applications. During ultrasonic modification of proteins, the cavitation effect generated at the ultrasonic probe can alter the structure of QP. The effect of variations in QP structure on protein function is not clarified. Therefore, by adjusting the ultrasound power levels, the effects of different power intensities on the structure and functionality of QP can be investigated.

To enhance the application of QP in the food industry, HIUS, a physical modification method, was introduced to modify QP. By adjusting the ultrasonic power, the structural changes of QP were investigated, and the effects of ultrasound on its foaming properties were thoroughly analysed, with the aim of improving the practical value of QP in the food industry.

Materials and methods

Materials

Quinoa was purchased from a local supermarket, and its protein was extracted with slight modifications to the method outlined by Cao *et al.* (2023), resulting in a purity of approximately 90.59%. All other reagents used in the present work were of analytical grade, and obtained from Tianjin Kaitong Reagent Co., Ltd.

HIUS processing of OP

The QP isolate powder was dispersed in deionised water to prepare a protein stock solution with a concentration of 5% (w/v) and pH 7.0. Subsequently, HIUS treatment was applied to the stock solution using an ultrasonic treatment

(sonicator, VCX500) at power levels of 0, 75, 150, 225, and 300 W for 10 min each, with a working time of 3 s followed by a 3 s pause. Finally, after freezedrying, HIUS-treated QP was obtained. The modified QP were designated as UQP-75, UQP-150, UQP-225, and UQP-300 based on the applied ultrasonic power levels (Yang *et al.*, 2024).

Particle size and ζ -potential of QP

The particle size and ζ -potential measurements of QP were conducted with slight modifications to the method outlined by Sow *et al.* (2019). Firstly, 1 mL of 0.2% (w/v) solution of QP was prepared, and changes in protein particle size and ζ -potential were analysed using a Zetasizer Nano Analyser (Zetasizer Nano ZS90, Thermo Fisher Scientific, USA), before and after ultrasonication (Song *et al.*, 2024).

Surface hydrophobicity (H_0) of QP

The hydrophobicity of QP was determined with some modifications to a previously established method (Huang et al., 2023). Initially, the sample was dissolved in a 0.01 mol/L phosphate buffer to prepare a 0.5 mg/mL solution. This solution was then mixed at a ratio of 5000:1 with a 0.008 mol/L ANS (1anilino-8-naphthalene sulfonate) solution, allowed to react for 2 min at 25°C. The fluorescence intensity of the mixed solution was measured at excitation and emission wavelengths of 390 and 468 nm, respectively, using fluorescence spectrophotometer (SpectraMax M5). A regression curve was obtained from the relative fluorescence intensity and protein concentration, with the slope (H₀) representing the surface hydrophobicity.

Free sulfhydryl (-SH) content of QP

Following the method outlined by Zou *et al.* (2020), the analysis of free thiol groups of QP before and after ultrasonication was conducted using Ellman's reagent (DTNB, 5,5'-dithiobis (2-nitrobenzoic acid)). Eq. 1 was used for calculating the free sulfhydryl content (µmol/g):

Free sulfhydryl content (
$$\mu$$
mol/g) = $\frac{73.53 \times A_{412} \times D}{C}$ (Eq. 1)

where, A = absorbance of QP solution, D = dilution factor of protein, and C = concentration of QP solution (mg/mL).

Fourier transform infrared spectra of QP

The secondary structure of QP was analysed using a Fourier-transform infrared (FTIR) spectrometer, specifically the Nicolet IS 10 from Thermo Fisher Scientific in Waltham, MA, USA.

The protein powder was mixed with KBr at a ratio of 100:1, and compressed into a pellet under a pressure of 50,000 N for subsequent measurements. The scanning conditions were set to 32 scans over a range of 4000 - 400 cm⁻¹.

The secondary structure of the protein was analysed using FTIR spectroscopy in the amide I region (1600 - 1700 cm⁻¹), which primarily reflects the C=O stretching vibrations of the peptide backbone. The spectrum was first baseline-corrected and smoothed using OMNIC software. Subsequently, second derivative and deconvolution analysis were performed using OriginPro and PeakFit to resolve overlapping peaks in the amide I region.

The deconvoluted peaks were fitted with Gaussian functions to assign specific wavenumber ranges to secondary structural elements: α-helix (typically 1648 - 1658 cm⁻¹), β-sheet (1618 - 1640 and 1670 - 1695 cm⁻¹), β-turn (1660 - 1670 cm⁻¹), and random coil (1640 - 1648 cm⁻¹). The area under each peak was calculated to estimate the relative content of each secondary structure type.

Fluorescence spectra of QP

With slight modifications to the method outlined by Li *et al.* (2016), the impact of HIUS on the fluorescence intensity of QP was analysed using Thermo Scientific Lumina (Thermo Fisher Scientific). A solution of 0.2 mg/mL QP was prepared in deionised water to measure the intrinsic tryptophan fluorescence intensity. Specifically, a slit width and excitation wavelength of 5 and 280 nm, respectively, were set, and the emission wavelength was set between 290 and 450 nm. The scanning voltage was 600 V, and the scanning speed was 100 nm/min.

Interfacial tension of OP

A protein solution was prepared with a concentration of 5 mg/mL, and the surface tension of QP was measured using a tensiometer (Sigma 700, Biolin) at 25°C.

Scanning electron microscopy of QP

The QP powder was immobilised on the sample stage using conductive adhesive, and then subjected to gold sputter coating under vacuum

conditions. Subsequently, the protein's microstructure was observed using a scanning electron microscope (SEM) (Inspect F50, FEI, Hillsboro, Oregon, USA) at an accelerating voltage of 5 kV (Song *et al.*, 2025). The magnification were 5000× and 10,000×.

Solubility of QP

Adopting the method proposed by Bradford (1976), the effect of HIUS on the solubility of QP was determined. Briefly, 1% (w/v) solutions of QP were prepared in deionised water. Subsequently, the solutions were centrifuged at 5,000 rpm for 15 min, and the supernatant was then collected to measure the dissolved protein content. This approach provided insights into how HIUS affected QP solubility using Eq. 2 (Wang *et al.*, 2025):

Solubility (%) =
$$\frac{m_1}{m} \times 100\%$$
 (Eq. 2)

where, m_1 = protein content in supernatant, and m = protein content in suspension.

Foaming properties of QP

The foam characteristics of QP typically include foam capacity (FC) and foam stability (FS). Following the method outlined by Li *et al.* (2016), a solution of 40 mL QP and 5 mg/mL UQP was prepared in deionised water, and denoted as V1. The solution was stirred at 13,800 rpm for 3 min, and the expanded volume after foaming was recorded as V2. After stabilising at room temperature for 30 min, the volume was recorded as V3. Subsequently, FC and FS were calculated using Eqs. 3 and 4:

FC (%) =
$$\frac{V_2 - V_1}{V_1} \times 100\%$$
 (Eq. 3)

FS (%) =
$$\frac{V_3 - V_1}{V_1} \times 100\%$$
 (Eq. 4)

Foam patterns in QP

Following the method outlined by Li *et al.* (2020), the differences in foam morphology between QP were observed using an IX73 fluorescence inverted microscope (OLYMPUS, Pooher Co., Ltd., Shanghai, China).

Protein content in QP by Kjeldahl method

The protein content of QP was determined using the Kjeldahl method following the AOAC Official Method 978.04, with slight modifications.

i) Digestion

Approximately 0.3 g of accurately weighed sample was placed into a digestion tube, followed by the addition of 10 mL concentrated sulphuric acid (H₂SO₄) and 0.5 g catalyst mixture (comprising potassium sulphate and copper sulphate in a 10:1 ratio). The mixture was heated at 380°C until the solution became clear, indicating complete digestion of organic matter.

ii) Distillation

After cooling, the digested solution was diluted with distilled water, and transferred into a distillation unit. A 40% (w/v) sodium hydroxide (NaOH) solution was added to render the medium strongly alkaline, liberating ammonia (NH₃), which was subsequently distilled and captured in 20 mL of 2% (w/v) boric acid solution containing a mixed indicator (methyl red and bromocresol green).

iii) Titration

The absorbed ammonia was titrated with standardised 0.1 mol/L hydrochloric acid (HCl) until the endpoint colour changed from green to pink. A reagent blank was simultaneously processed under identical conditions.

iv) Calculation

The nitrogen content was calculated based on the volume of HCl consumed, and the protein content was obtained by multiplying the nitrogen content by a conversion factor of 6.25. The result was expressed as a percentage of dry weight using Eq. 5:

Protein (%) =
$$\frac{(v_{sample}-v_{blank}) \times C \times 14.007 \times 6.25}{W \times 1000} \times 100$$
(Eq. 5)

where, V_{sample} = volume of HCl used for the sample (mL), V_{blank} = volume of HCl used for the blank (mL), C = concentration of HCl (mol/L), and W = weight of the sample (g).

Statistical analysis

The data were statistically analysed using SPSS software (version 22) with one-way ANOVA, and the results were presented as mean and standard deviation. A significance level of 0.05 was set for statistical significance. Graphs representing the data were created using SigmaPlot 11.0 and Origin 2018.

Results and discussion

 ζ -potential and particle size of QP

Figures 1A and 1B depict the ζ -potential and particle size of QP, respectively. From Figure 1A, a significant increase in the absolute value of QP's ζ -potential can be seen with increasing ultrasound power, indicating a substantial enhancement in the charge carried by QP. As shown in Figure 1A, the absolute value of the ζ -potential of QP significantly increases with increasing ultrasonic power, from an initial value of 17.85 to 38.54 mV, indicating a substantial increase in the surface charge of QP.

Simultaneously, as shown in Figure 1B, the particle size of QP significantly decreases from the initial value of 847.37 to 351.86 nm. The decrease in protein particle size could be attributed to the cavitation effect generated by the ultrasound probe, disrupting non-covalent bonds between protein molecules, and breaking down soluble aggregates into smaller fragments. During this process, charged groups within the protein become more exposed, leading to the observed increase in ζ -potential. Protein particle size is not only a crucial indicator affecting protein solubility, but also influencing key functional properties such as foaming emulsification. Previous studies, such as on perilla protein isolate, have reported that ultrasound significantly improved protein solubility, foam stability, and emulsification stability by reducing particle size (Zhao et al., 2022a).

Hydrophobicity (H_0)

Hydrophobicity is a critical parameter influencing protein interfacial properties (Huang *et al.*, 2025a). Figure 1C illustrates the hydrophobicity of QP under ultrasound treatment. With an increase in ultrasound power, QP's hydrophobicity significantly improved, reaching its maximum value at 300 W. This increase could be attributed to structural changes in QP's tertiary structure under ultrasound influence, leading to unfolding and exposing hydrophobic groups internally. Experiments by Meng *et al.* (2021) similarly found an increase in the hydrophobicity of whey protein isolate following ultrasound treatment.

Free sulfhydryl (-SH) content of QP

Changes in protein-free thiol groups are typically associated with disulphide bonds, and reflect alterations in protein tertiary structure.

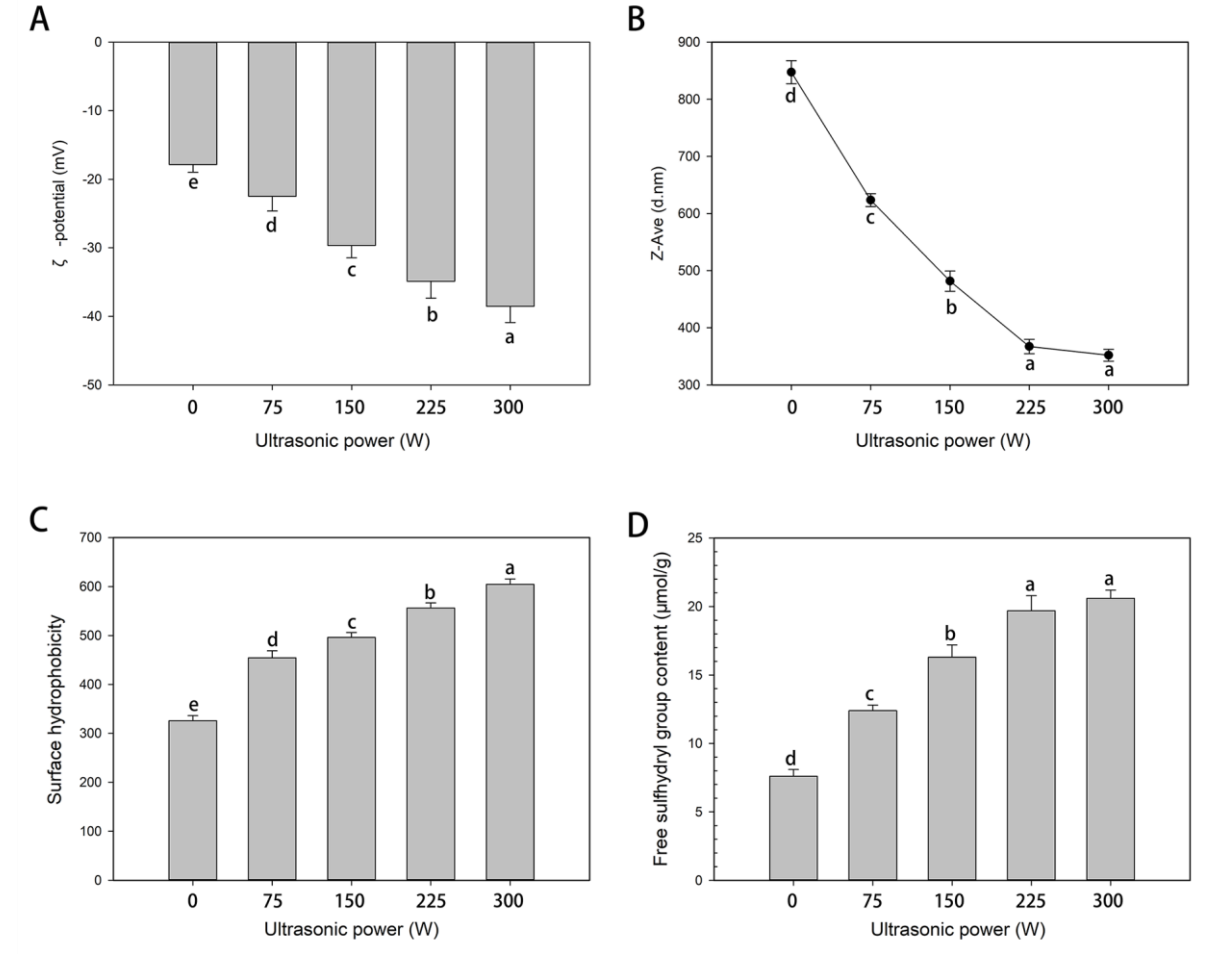


Figure 1. (A) ζ-point, (B) particle size, (C) surface hydrophobic, and (D) free sulfhydryl content of quinoa protein. Different lowercase letters indicate significant difference (p < 0.05) between samples.

In Figure 1D, QP's free thiol content shows a significant increase as the ultrasound power increases, increasing from the initial value of 8.7 to 22.5. Under ultrasound influence, QP's tertiary structure underwent changes, thus opening up the protein structure, and exposing internal -SH groups to the surface.

Infrared spectroscopy

Figure 2A displays the Fourier transform infrared (FTIR) spectra of native and modified QP under various ultrasonic power levels (UQP-75, UQP-150, UQP-225, and UQP-300). All samples exhibited typical absorption bands corresponding to protein functional groups, with notable changes observed as ultrasonic power increased.

The broad band around 3280 cm⁻¹ is assigned to O–H and N–H stretching vibrations, primarily reflecting intramolecular and intermolecular hydrogen bonding and amide A structures. This peak became broader, and slightly shifted to lower

wavenumbers with increasing ultrasonic intensity, suggesting enhanced exposure of polar groups, and stronger hydrogen bonding due to partial unfolding of the protein structure.

The amide I band (centred at $\sim 1640~\text{cm}^{-1}$), primarily resulting from C=O stretching vibrations of the peptide backbone, is sensitive to secondary structure. With increasing ultrasonic power, this peak showed a gradual shift and increased intensity, indicating alterations in protein conformation, particularly a transition in the relative contents of α -helix and β -sheet structures. These changes reflected protein unfolding and reorganisation of the hydrogen bond network within the backbone.

The amide II band (~1535 - 1545 cm⁻¹), attributed to N–H bending and C–N stretching, also increased in intensity under higher ultrasonic powers, implying that ultrasound treatment enhanced the mobility or exposure of internal peptide bonds, and altered the local protein environment.

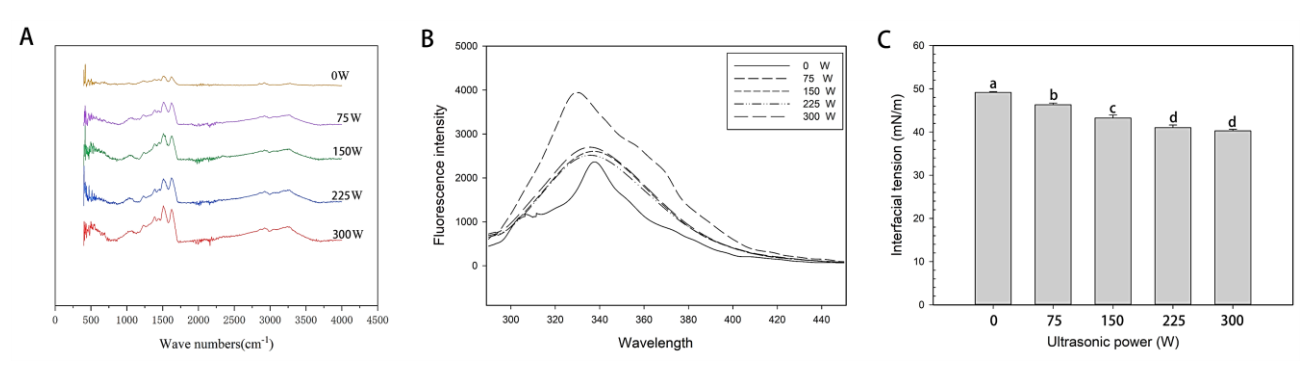


Figure 2. (A) FTIR, (B) fluorescence spectrum, and (C) interfacial tension of quinoa protein.

A noticeable increase was also observed in the peak at ~1400 cm⁻¹, assigned to C-H bending vibrations, which may reflect rearrangement or increased exposure of side chains. Moreover, the peak at ~1070 cm⁻¹, corresponding to C-O stretching vibrations of alcohol or carbohydrate-like moieties, showed enhancement and slight shifts, suggesting ultrasonic disruption of side chain packing, and possible interactions with residual glycosidic components.

Infrared analysis of QP's secondary structure, as shown in Table 1, revealed an increase in QP's α -helix content from the initial value of 22.86 to 28.12, while β -sheet and β -turn decreased from 32.01 and 24.07 to 28.31 and 20.25. The decrease in β -sheet content, as the most tightly connected structure in proteins, may be attributed to the shearing and cavitation effects produced by ultrasound, disrupting its compact structure and altering its secondary structure.

Table 1. Secondary structure composition of quinoa protein.

Ultrasonic	Secondary structure (%)			
power (W)	α-helix	β-turn	β-sheet	Random coil
0	22.86 ± 0.2^a	32.01 ± 0.2^e	24.07 ± 0.2^e	$22.78 \pm 0.1^{\text{b}}$
75	22.91 ± 0.1^a	$31.54 \pm 0.1^{\text{d}}$	23.17 ± 0.2^{d}	22.86 ± 0.2^a
150	24.21 ± 0.2^{b}	30.40 ± 0.1^{c}	22.39 ± 0.1^{c}	$22.82 \pm 0.2^{\text{b}}$
225	25.74 ± 0.2^{b}	29.21 ± 0.2^{b}	21.26 ± 0.1^{b}	23.14 ± 0.1^{ab}
300	28.12 ± 0.3^{c}	28.31 ± 0.1^{a}	20.25 ± 0.2^a	23.07 ± 0.2^{b}

Data are mean \pm standard deviation. Different lowercase superscripts in similar column indicate significant difference in secondary structure between ultrasonic powers (p < 0.05).

Fluorescence spectroscopy

Fluorescence spectroscopy results further corroborated the changes in protein tertiary structure. As shown in Figure 2B, with the increase in ultrasound intensity, the fluorescence intensity of the protein also significantly increase. When the ultrasound intensity reached 300 W, UQP-300 exhibited the highest fluorescence intensity. This may be due to the decrease in particle size in the solvent, and the increased solubility of the protein, leading to the exposure of many chromophores. In addition, the unfolding of the QP structure exposed tryptophan and tyrosine residues, which also contributed to this phenomenon. In addition to the increase in fluorescence intensity, a red shift was also observed,

which may indicate the exposure of hydrophilic groups after the change in the tertiary structure of QP. Similar phenomena were observed in experiments involving watermelon seed protein (Wen *et al.*, 2019). Moreover, the fluorescence spectrum of unmodified QP exhibited multiple irregular peaks, which may be due to the presence of many soluble aggregates in the protein that had not undergone HIUS treatment.

Interfacial tension

Interfacial tension is a crucial indicator affecting protein foam properties, representing the interface properties of the protein-water-air interface. As shown in Figure 2C, QP's interfacial tension

significantly decreases from 49.17 to 40.26 with increasing ultrasound power. This decrease may be influenced by QP's ζ -potential. A higher surface charge can enhance interfacial stability by reducing surface tension through electrostatic repulsion, and inhibiting bubble coalescence, which contributes to the formation of a more stable foam system. Generally, lower interfacial tension is advantageous for enhancing protein's interfacial activity at the water-air interface, contributing to the stabilisation of more foam (Meng *et al.*, 2024).

Scanning electron microscopy (SEM)

Figure 3 displays the SEM images of QP, providing a more intuitive observation of the impact of ultrasound on QP's microstructure (Huang *et al.*, 2025b). As the ultrasound power increased, the pores between protein particles became denser, resulting in a more uniform particle size and morphology. This observation aligned with the conclusions drawn from particle size analysis (Yan *et al.*, 2023).

Solubility

Solubility is fundamental a property influencing the further application of proteins. From Figure 4A, it can be seen as the ultrasound power increases, QP's solubility significantly improves from the initial value of 10.59 to 57.86. The substantial decrease in protein particle size and changes in secondary and tertiary structures, as observed in earlier experiments, played a crucial role in enhancing protein solubility. Additionally, the disruption of soluble aggregates by the shear and cavitation forces of ultrasound also contributed to the increased solubility of the protein.

Foaming capacity (FC) and foam stability (FS)

Foaming capacity, as a critical property for protein resource utilisation, has gained widespread attention in recent years. Due to its low solubility, QP's foaming capacity has not met the requirements of food processing. As seen in Figures 4B and 4C, with increasing ultrasound intensity, QP's foaming capacity and foam stability significantly improve, reaching their maximum values (107.24%) at 300 W. In addition, to comprehensively characterise foam stability, the stability of QP foam after 2 h was evaluated. As shown in Figure 4D, after a 2 h observation period, the foam stability of UQP-300 remains significantly higher (32.18%) than that of QP

and the other treatment groups. Changes in protein foaming capacity are influenced by various factors, including the decrease in particle size, the disruption of soluble aggregates leading to smaller particle size, and increased protein quantity at the water-air interface, resulting in improved foam stability. The increase in surface hydrophobicity, and the decrease in surface tension also affect foam capacity, with higher hydrophobicity facilitating protein adsorption at the water-air interface, and lower interfacial tension enhancing the protein's stability at the interface, ultimately forming stable foam (Zhao *et al.*, 2022b).

Microscopic images of QP foam

To further confirm QP's foam stability, a microscopic analysis of the obtained foam was conducted using a fluorescence inverted microscope. As shown in Figure 5, untreated protein forms larger foam with thinner walls. With the increase in ultrasound power, the foam volume stabilised by QP gradually decreased, while the foam walls became progressively thicker. When the ultrasound power reached 300 W, the resulting foam exhibited the smallest volume, and the thickest foam walls. In contrast, under ultrasound influence, QP's foam not only exhibited reduced size, but also thicker walls. Smaller foam size and thicker walls contributed to improved foam stability, aligning with conclusions mentioned previously in section "Foaming capacity (FC) and foam stability (FS)" (Huang et al., 2024).

Conclusion

Due to the inherently poor water solubility of quinoa protein (QP), its foaming capacity in the food industry is significantly limited. In the present work, high-intensity ultrasound (HIUS) was applied to modify QP in order to address this issue. The effects of ultrasound treatment on the fundamental properties, secondary structure, and tertiary structure of QP were systematically investigated, and the resulting changes were correlated with improvements in solubility and foaming capacity. Following ultrasonic treatment, the particle size of QP decreased from 847.37 to 351.86 nm, and notable alterations in its secondary structure were observed. Specifically, the α -helix content increased from 22.86 to 28.12%, while the β -sheet content decreased from 24.07 to

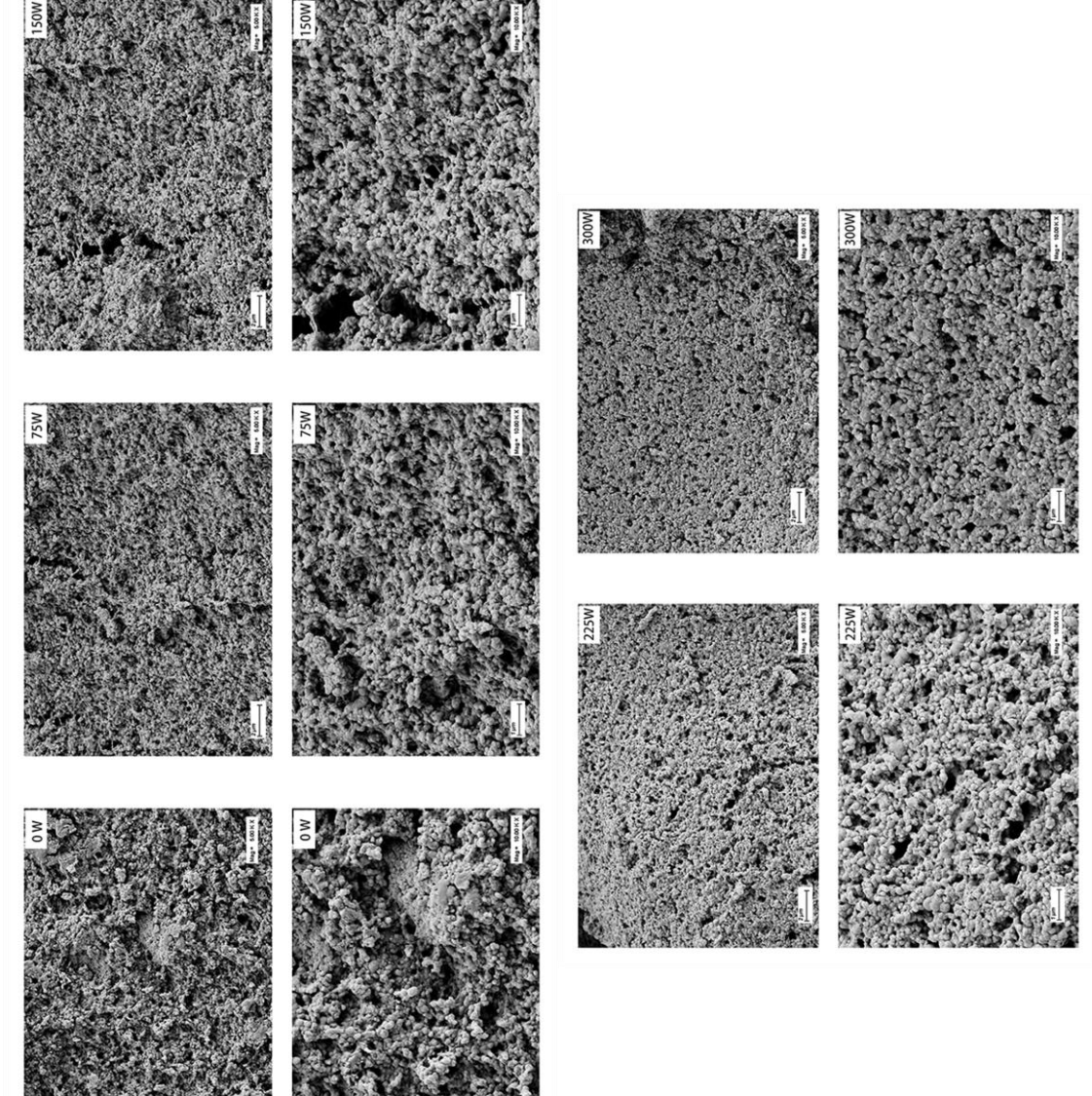


Figure 3. Scanning electron microscope image at $5000 \times$ and $10,000 \times$ magnifications.

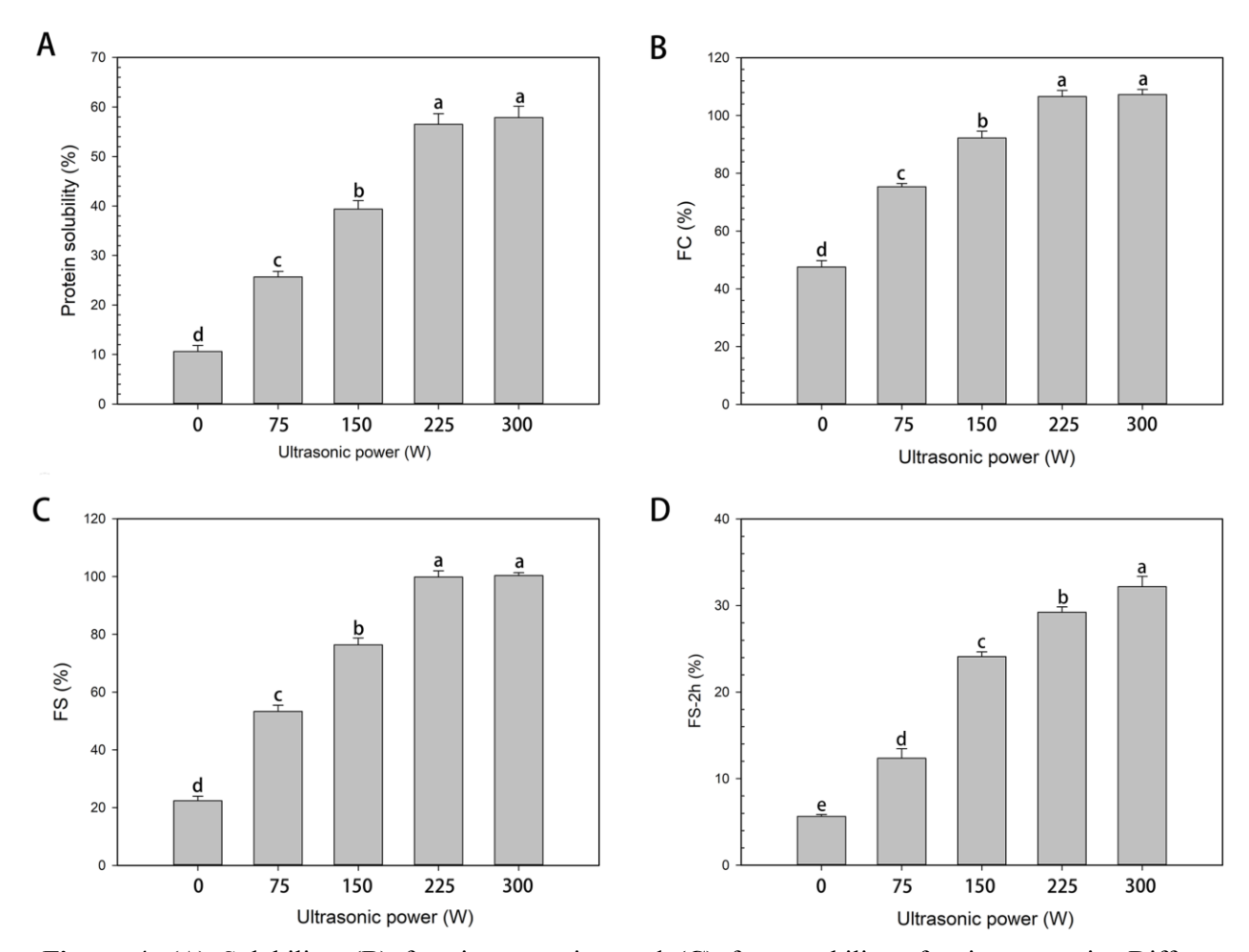


Figure 4. (A) Solubility, **(B)** foaming capacity, and **(C)** foam stability of quinoa protein. Different lowercase letters indicate significant difference (p < 0.05) between samples.

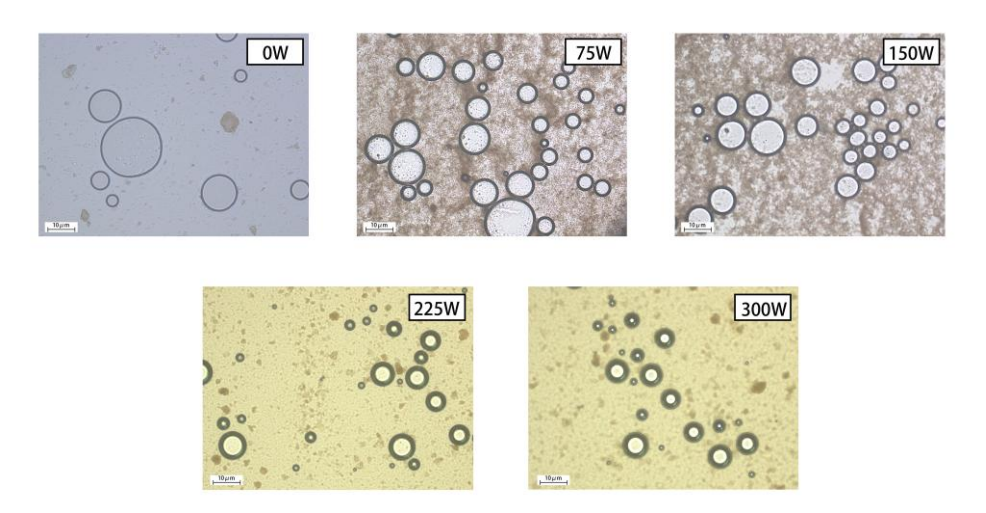


Figure 5. Microscopic images of foams created by quinoa protein.

20.25%. These structural and morphological modifications led to significant enhancements in the functional properties of QP. At an ultrasound power of 300 W, QP exhibited the highest solubility, reaching 57.86%. Furthermore, the foaming properties of QP improved progressively with increasing ultrasound power, with the foaming capacity increasing from 47.56 to 107.24%. These findings demonstrated that HIUS could be an effective strategy for improving the foaming functionality of QP, offering promising potential for its application in the food industry.

References

- Bradford M. M. 1976. A rapid and sensitive method for the quantitation of microgram quantities of protein utilizing the principle of protein-dye binding. Analytical biochemistry 72: 248-254.
- Cao, H., Huang, Q., Shi, J., Guan, X., Song, H., Zhang, Y., ... and Fang, Y. 2023. Effect of conventional and microwave heating treatment on antioxidant activity of quinoa protein after simulated gastrointestinal digestion. Food Chemistry 415: 135763.
- Cui, H., Li, S., Roy, D., Guo, Q. and Ye, A. 2023. Modifying quinoa protein for enhanced functional properties and digestibility: A review. Current Research in Food Science 7: 100604.
- Du, H., Zhang, J., Wang, S., Manyande, A. and Wang, J. 2022. Effect of high-intensity ultrasonic treatment on the physicochemical, structural, rheological, behavioral, and foaming properties of pumpkin (*Cucurbita moschata* Duch.)-seed protein isolates. LWT Food Science and Technology 155: 112952.
- Fu, J., Ren, Y., Jiang, F., Wang, L., Yu, X. and Du, S.-K. 2022. Effects of pulsed ultrasonic treatment on the structural and functional properties of cottonseed protein isolate. LWT Food Science and Technology 172: 114143.
- Huang, D., Hao, R., Zhang, W., Liu, Y., Lin, X., Song, W., ... and Li, D. 2025b. High-intensity ultrasound-modified Jerusalem artichoke leaf protein for stabilizing corn oi-in-water emulsion and enhancing curcumin delivery. Food Chemistry 463: 141240.
- Huang, D., Li, W., Li, G., Zhang, W., Chen, H., Jiang, Y. and Li, D. 2023. Effect of high-intensity ultrasound on the physicochemical properties

- of Tenebrio Molitor Protein. Food Hydrocolloids 134: 108056.
- Huang, D., Xu, Y., Zhang, W., Liu, Y., Zhang, T., Liu, H., ... and Li, D. 2024. Enhancement of foaming property of ormosia protein: Insights into the effect of high-intensity ultrasound on physicochemical properties and structure analysis. Food Hydrocolloids 152: 109902.
- Huang, D., Zhang, W., Liu, Y., Zhang, J., Jiang, Y., Huang, Q. and Li, D. 2025a. Effect of combined pH-shifting and high-intensity ultrasound treatment on the structural, functional, and foaming properties of Tenebrio Molitor Protein. Food Hydrocolloids 167: 111384.
- Kong, Y., Sun, L., Wu, Z., Li, Y., Kang, Z., Xie, F. and Yu, D. 2023. Effects of ultrasonic treatment on the structural, functional properties and beany flavor of soy protein isolate: Comparison with traditional thermal treatment. Ultrasonics Sonochemistry 101: 106675.
- Li, K., Fu, L., Zhao, Y.-Y., Xue, S.-W., Wang, P., Xu, X.-L. and Bai, Y.-H. 2020. Use of high-intensity ultrasound to improve emulsifying properties of chicken myofibrillar protein and enhance the rheological properties and stability of the emulsion. Food Hydrocolloids 98: 105275.
- Li, S., Yang, X., Zhang, Y., Ma, H., Liang, Q., Qu, W., ... and Mahunu, G. K. 2016. Effects of ultrasound and ultrasound assisted alkaline pretreatments on the enzymolysis and structural characteristics of rice protein. Ultrasonics Sonochemistry 31: 20-28.
- Meng, Y., Liang, Z., Zhang, C., Hao, S., Han, H., Du,
 P., ... and Liu, L. 2021. Ultrasonic modification of whey protein isolate:
 Implications for the structural and functional properties. LWT Food Science and Technology 152: 112272.
- Meng, Y., Wei, Z. and Xue, C. 2024. Correlation among molecular structure, air/water interfacial behavior and foam properties of naringin-treated chickpea protein isolates. Food Hydrocolloids 147: 109309.
- Nasrabadi, M. N., Doost, A. S. and Mezzenga, R. 2021. Modification approaches of plant-based proteins to improve their techno-functionality and use in food products. Food Hydrocolloids 118: 106789.

- Song, G., Li, F., Xu, Z., Jiang, N., Wang, D., Yuan, T., ... and Gong, J. 2025. Exploring the noncovalent interaction between β-lactoglobulin and flavonoids under nonthermal process: Characterization, physicochemical properties, and potential for lycopene delivering. Food Chemistry X 25: 102160.
- Song, G., Zhou, L., Zhao, L., Wang, D., Yuan, T., Li, L. and Gong, J. 2024. Analysis of non-covalent interaction between β-lactoglobulin and hyaluronic acid under ultrasound-assisted treatment: Conformational structures and interfacial properties. International Journal of Biological Macromolecules 256: 128529.
- Sow, L. C., Toh, N. Z. Y., Wong, C. W. and Yang, H. 2019. Combination of sodium alginate with tilapia fish gelatin for improved texture properties and nanostructure modification. Food Hydrocolloids 94: 459-467.
- Wang, F., Dai, S., Ye, J., Yang, X., Xu, J., Zhang, S., ... and Deng, G. 2025. Soy protein isolate/dextran glycation conjugates: Fabrication through ultrasound-assisted cyclic continuous reaction and their applications as carriers of anthocyanins. International Journal of Biological Macromolecules 294: 139485.
- Wang, S., Miao, S. and Sun, D.-W. 2024. Modifying structural and techno-functional properties of quinoa proteins through extraction techniques and modification methods. Trends in Food Science and Technology 143: 104285.
- Wen, C., Zhang, J., Zhang, H., Duan, Y. and Ma, H. 2019. Effects of divergent ultrasound pretreatment on the structure of watermelon seed protein and the antioxidant activity of its hydrolysates. Food Chemistry 299: 125165.
- Yan, J., Zhao, S., Xu, X. and Liu, F. 2023. Enhancing pea protein isolate functionality: A comparative study of high-pressure homogenization, ultrasonic treatment, and combined processing techniques. Current Research in Food Science 8: 100653.
- Yang, C., Zhu, X., Huang, J., Wei, Y., Wen, L., Yang, F., ... and Liu, W. 2024. Harnessing ultrasonic power to optimize quinoa byproduct protein for sustainable utilization. LWT Food Science and Technology 207: 116629.
- Yang, J., Duan, Y., Geng, F., Cheng, C., Wang, L., Ye, J., ... and Deng, Q. 2022. Ultrasonic-assisted pH shift-induced interfacial remodeling for enhancing the emulsifying and

- foaming properties of perilla protein isolate. Ultrasonics Sonochemistry 89: 106108.
- Zhao, Q., Xie, T., Hong, X., Zhou, Y., Fan, L., Liu, Y. and Li, J. 2022a. Modification of functional properties of perilla protein isolate by high-intensity ultrasonic treatment and the stability of o/w emulsion. Food Chemistry 368: 130848.
- Zhao, X., Fan, X., Shao, X., Cheng, M., Wang, C., Jiang, H., ... and Yuan, C. 2022b. Modifying the physicochemical properties, solubility and foaming capacity of milk proteins by ultrasound-assisted alkaline pH-shifting treatment. Ultrasonics Sonochemistry 88: 106089.
- Zou, H., Zhao, N., Sun, S., Dong, X. and Yu, C. 2020. High-intensity ultrasonication treatment improved physicochemical and functional properties of mussel sarcoplasmic proteins and enhanced the stability of oil-in-water emulsion. Colloids and Surfaces A - Physicochemical and Engineering Aspects 589: 124463.